communications earth & environment

Article

A Nature Portfolio journal

https://doi.org/10.1038/s43247-026-03601-0

Reversing methanogenesis to produce ethanol

Ruchira Mitra[1], Yunjeong Choi[1], Hyeon-Ji Hwang[1], Rodolfo García-Contreras[1,2], Vanesa Angarita-Zapata[1], Shotaro Toya[1], Ilke Gurgan[1], Ingmar H. Riedel-Kruse[3,4] & Thomas K. Wood[1]

Capturing greenhouse gases and converting them into biochemicals is beneficial. Previously, we reversed methanogenesis by cloning methyl-coenzyme M reductase (Mcr) from an unculturable population of anaerobic methanotrophic archaea into the methanogen *Methanosarcina acetivorans* to capture both methane and carbon dioxide to produce acetate, lactate, and electricity. In the present study, we found that the methane captured (130 ± 30 µmol) by ANME-1 Mcr in *M. acetivorans* is converted from acetate to ethanol (120 ± 10 µmol). Moreover, ethanol production was tripled (370 ± 20 µmol) by adding iron(III) and humic acids to facilitate electron transfer and yeast extract to stimulate growth. We further introduced heterologous carboxylic acid reductase and alcohol dehydrogenase into the same host with the goal to produce even more ethanol from the intermediate acetate, but we found that this actually leads to a drop in ethanol yield, showing that the methanogenic host converts acetate from Mcr-captured methane by utilizing its native aldehyde ferredoxin oxidoreductase and alcohol dehydrogenase. Hence, we demonstrate that *M. acetivorans* may be utilized to produce ethanol from methane and carbon dioxide, that this conversion is enhanced by heterologous production of ANME-1 Mcr, and that the host can produce ethanol from acetate.

Carbon dioxide is the most-abundant greenhouse gas[1], emitted at 42 Gt/yr[2]; hence, its emissions need to be reduced. Methane is also a potent greenhouse gas that is emitted at ~0.58 Gt/yr, has a 28-fold more global warming potential per molecule relative to CO_2[3], and human emitted green-house gases are currently projected to cause more than a 3 °C increase in global temperatures by the end of the 21st century[1]. Both methanotrophs (aerobically) and anaerobic methanotrophic archaea (ANME) capture methane; however, the ANME process dominates with aerobic methane oxidation at ~30 Tg/yr[1] and anaerobic methane oxidation at up to ~300 Tg/yr[4]. Furthermore, methane capture via oxidation is one of the 'Holy Grails' of catalysis[1], and anaerobic oxidation of methane has many applications and is more efficient than aerobic processes[3].

Unfortunately, ANME cannot be grown as pure cultures[1,4]; hence, we previously cloned the ANME-1 *mcrBGA* genes (3.9 kb) encoding Mcr from Black Sea sediments, where ANME rates are the highest measured[4], into the methanogen *Methanosarcina acetivorans*[5], to produce active ANME-1 Mcr that captures both methane and carbon dioxide and converts them to acetate[6], allowing growth on methane by an anaerobic pure culture. This host was chosen since it is both genetically tractable[7] and contains the necessary cofactors and enzymes required for reversing methanogenesis[6]; note that this host has its own version of Mcr, optimized for the reverse reaction from acetate to methane, and in the following we refer to 'host Mcr' and 'ANME-1 Mcr', respectively. The resulting stoichiometry for reversed methanogenesis using ferric iron to accept the electrons required for oxidizing fully-reduced methane[6] is

$$4CH_4 + 2HCO_3^- + 8Fe^{3+} + 3ADP + 3P_i \rightarrow 3CH_3COO^- + 8Fe^{2+} + 9H^+ + 3ATP\ \Delta G^{\circ\prime} = -593.1\text{kJ/mol} \quad (1)$$

This approach[6] allows active ANME-1 Mcr to be studied for the first time and mimics how ANME evolved by reversing methanogenesis[8].

The recombinant *M. acetivorans* system producing ANME-1 Mcr that reverses methanogenesis was also utilized previously to produce *L*-lactate from methane by cloning 3-hydroxybutyryl-CoA dehydrogenase (Hbd) from *Clostridium acetobutylicum*[9]. The yield with this strain was 10-fold higher compared to aerobic approaches[9], and lactic acid may be used in

[1]Department of Chemical Engineering, Pennsylvania State University, University Park, Pennsylvania, USA. [2]Department of Microbiology and Parasitology, Faculty of Medicine, National Autonomous University of Mexico, Mexico City, Mexico. [3]Department of Molecular and Cellular Biology, University of Arizona, Tucson, AZ, USA. [4]Departments of Applied Mathematics, Biomedical Engineering, and Physics, University of Arizona, Tucson, AZ, USA. e-mail: tuw14@psu.edu

cosmetics[10], in foods[11], in pharmaceuticals[12], and in bio-degradable plastics[13].

By reversing methanogenesis with ANME-1 Mcr, the first biological fuel cell that converts methane into electricity was created[14,15]. Critically, this microbial fuel cell[14,15] has high Coulombic efficiency and produces electricity as well as any non-gas substrate, achieving 5.2 W/m^2 and 7 A/m^2.

Here, we cloned *mcrBGA* encoding Mcr from the ANME-1 Black Sea metagenome, *car* encoding carboxylic acid reductase (Car) from *Moorella thermoacetica*, and *adh* encoding alcohol dehydrogenase (Adh) from *Synechocystis* sp. PCC 6803 to convert captured methane and carbon dioxide to ethanol in *M. acetivorans*. Surprisingly, we found that the acetate formed from the ANME-1 Mcr-captured methane is readily converted to ethanol, probably via the aldehyde ferredoxin oxidoreductase (AOR) and Adh of the methanogenic host, while the cloned *car* and *adh* were detrimental.

Methods

Culture conditions

The strains used are shown in Supplementary Table S1. *M. acetivorans* C2A (DSMZ Collection #2834) was routinely grown anaerobically at 39 °C in 100 mL of sterile 50 mM 1,4-piperazinediethanesulfonic acid (PIPES) buffered- high salt (HS) medium[6] with 2.5 g/L yeast extract (HSYE) supplemented with 0.5% v/v methanol as the carbon source, 0.025% w/v $Na_2S{\cdot}9H_2O$ as the reducing agent, and 2 μg/mL puromycin for maintaining plasmid[6]. The pH of the medium was 6.5. A thawed 1.8 mL aliquot of each glycerol stock was inoculated into 100 mL of HSYE medium in an anaerobic chamber, the bottles were sealed, and cultures were incubated at 200 rpm for 10 to 15 days to a turbidity at 600 nm of approximately 0.5. Experiments on methane were done as previously described[6], except that the medium was buffered with 50 mM PIPES. Cells on methanol were harvested to a target density of ~4×10^{10} cells/mL (turbidity 40) by centrifugation at 5,000 rpm for 20 min. The cell pellet was washed three times to remove residual methanol with either HS medium (when HS medium was used for growing cells on methane) or HSYE medium (when HSYE medium was used for growing cells on methane) containing 3.8 g/L sodium carbonate, 0.025% w/v $Na_2S{\cdot}9H_2O$, and 2 μg/mL puromycin. Washed cell pellets were then resuspended in 12 mL of either HS or HSYE medium containing 3.8 g/L sodium carbonate, 0.025% w/v $Na_2S{\cdot}9H_2O$ and 2 μg/mL of puromycin in 40 mL crimp-sealed glass vials, and the turbidity was adjusted to ≈ 40. Where indicated, freshly prepared and filter-sterilized (0.22 μm) $FeCl_3$ (10 mM) and humic acids (0.1 g/L) were added. The liquid phase was sparged with 99% of methane at 70 mL/min for 5 min using both inlet and outlet needles to allow continuous gas exchange and to prevent pressure buildup. The headspace (28 mL) was fully replaced with methane, and the pressure was maintained at atmospheric pressure. The sealed vials were then incubated inverted at 250 rpm.

Construction of pES1-EtOH

pES1-EtOH (Supplementary Fig. S1) was constructed by GenScript USA, Inc (Piscataway, NJ, USA) from pES1-MAT*mcr3*[6] by cloning *car* from *Moorella thermoacetica* and *adh* from *Synechocystis* sp. PCC 6803 under control of methane-induced $P_{mcr\_ANME\text{-}1}$ promoter ($P_{mcr\_ANME\text{-}1}$::*car* and $P_{mcr\_ANME\text{-}1}$::*adh*). The plasmid was then electroporated anaerobically into *Escherichia coli* DH5α (λ pir), and purified pES1-EtOH was verified by sequencing by Plasmidsaurus (Louisville, KY, USA).

Transformation of *M. acetivorans*

All plasmids (pES1-MAT*mcr3*, pES1(Pmat), and pES1-EtOH) were transformed into *M. acetivorans* by electroporation under anaerobic conditions. Cells were grown in HSYE medium (with 0.5% v/v methanol and 0.025% w/v $Na_2S{\cdot}9H_2O$) to a turbidity at 600 nm of 1.0. Cells (10 mL) were harvested by centrifugation at 8000 rpm for 15 min and washed twice in same volume of cold (0°C) 0.85 M sucrose. Washed cells were resuspended with 100 μL of cold 0.85 M sucrose and mixed with 5 μg of plasmid DNA. The mixture was transferred into a cold electroporation cuvette, electroporated (1.25 kV, 200 Ω, and 25 μF using a Biorad Gene Pulser apparatus, model number: 165-2098), and mixed with 900 μL HSYE medium (with 0.5% v/v methanol and 0.025% w/v $Na_2S{\cdot}9H_2O$). The cell suspension was then transferred to 3 to 5 mL HSYE medium (with 0.5% v/v methanol and 0.025% w/v $Na_2S{\cdot}9H_2O$) and incubated at 39 °C for 24 h for recovery; note that growth as colonies on solid medium was not possible. The cells were harvested by centrifugation and resuspended with 10 mL HSYE medium (with 0.5% v/v methanol, 0.025% w/v $Na_2S{\cdot}9H_2O$ and 2 μg/mL puromycin) and incubated at 39 °C for 5 to 7 days to obtain the transformed cells. Transformation was validated by polymerase chain reaction (PCR) of the puromycin resistance gene present in the plasmid backbone using the forward primer 5'-CAGCAACAGATGGAAGGCC-3' and the reverse primer 5'-TCGTAGAAGGGGAGGTTGC-3'.

Total protein

Total protein was quantified using the Bradford assay (Bio-Rad Laboratories, Hercules, CA, USA). Sample (100 μL) was harvested by centrifugation at 6000 g for 5 min, and the supernatant and cell pellet were separated. Cell pellets were resuspended in distilled water to a final volume of 100 μL, vortexed for 30 sec, and heated at 90 °C for 60 min to lyse cells. Supernatants and the lysate suspensions (diluted with distilled water) were transferred to a 96-well plate and mixed with 200 μL of 1× Bradford reagent. After 40 s of shaking, the absorbance was measured at 595 nm. A calibration curve was generated with bovine serum albumin (BSA) standards, and protein concentrations were calculated from the linear regression of A_{595} versus BSA concentration.

Methane, ethanol, and acetate assays via gas chromatography

All GC analyses were performed on an Agilent 6890 N gas chromatograph using nitrogen as the carrier gas. Headspace methane was analyzed with a Carboxen-1000 packed column (4600 × 2.1 mm, Supelco catalog no. 12390-U) and a thermal conductivity detector (TCD). Injections were 30 μL of headspace. The front inlet and detector were maintained at 150 °C and 240 °C, respectively. The column temperature was initially set at 185 °C, then increased to 220 °C at a rate of 16 °C/min and held at 230 °C for 6 min. Nitrogen served as both carrier and reference gas. Flow rate for detector gas was kept at 20 mL/min. Gases were identified according to their retention times and their concentrations were determined according to comparisons with standards.

Ethanol was assayed with a 0.1% AT-1000 packed column (6′, 1/8″ O.D., 80/100 mesh on Graphpac-GC support; Alltech) and a flame ionization detector (FID). The front inlet and detector were maintained at 150 °C and 210 °C, respectively. The column temperature was initially set at 50 °C for 1 min, then increased to 220 °C at a rate of 50 °C/min and held for 2 min. The supernatant (2 μL) of samples harvested by centrifugation at 8000 g for 8 min was injected. Concentrations were calculated from calibration curve. Standard solutions for ethanol were prepared using the same medium composition as in the experiments.

Acetate was assayed using a Stabilwax-DA capillary column (30 m × 0.53 mm i.d., 0.25 μm film; Restek) with FID detection. The oven program was 70 °C hold, 40 °C/min to 100 °C, 100 °C/min to 200 °C. The front inlet and detector were set to 250 °C. For sample preparation, culture was centrifuged at 8,000 rpm for 8 min, and 100 μL supernatant was acidified with 1 μL formic acid. The acidified supernatant (2 μL) was injected. Calibration curves were prepared with sodium acetate standards in different conditions matching the test media, and matrix-matched calibration was applied for quantitation. All GC sample injections were performed manually in triplicates using a high-precision syringe (Hamilton Co., Reno, NV, USA) to ensure precise and reproducible peak area.

Statistical analysis

Statistical analysis was performed using GraphPad Prism 10. Data are presented as the mean ± standard deviation (SD) of at least three independent cultures. Student's T-test was performed to evaluate the difference between data sets, with probability values (p) <0.05 considered significant.

Reporting summary

Further information on research design is available in the Nature Portfolio Reporting Summary linked to this article.

Results

Rationale

We hypothesized that the *M. acetivorans* C2A (henceforth 'C2A') chassis engineered to capture methane and carbon dioxide via ANME-1 Mcr[6] for producing the biofuel precursor, acetate, C2A/pES1-MAT*mcr3* (Supplementary Fig. S1A), could be further used to convert this acetate to ethanol. Therefore, we assayed ethanol production by C2A/pES1-MAT*mcr3* and compared it to the empty vector control C2A/pES1(Pmat) (Supplementary Fig. S1B). We used high-cell density cultures with turbidity of 40 at OD_{600} with methane in the headspace[6] so that we could readily assay chemical transformations after 6 days of anaerobic incubation. In addition, vials without cells were used to estimate the amount of ethanol produced abiotically. We then maximized the ethanol production by supplementing with external electron acceptor iron(III), yeast extract, humic acids, and glass wool. Finally, we attempted to further engineer the strain to increase ethanol production by adding genes for heterologous carboxylic acid reductase and alcohol dehydrogenase.

ANME-1 Mcr increases ethanol production by *M. acetivorans*

With ANME-1 Mcr, ethanol was produced at 120 ± 10 µmol by C2A/pES1-MAT*mcr3* whereas C2A/pES1(Pmat) produced 50 ± 20 µmol, after 6 days of incubation (Fig. 1A). Similarly, normalized ethanol production was 2.5-fold higher (5.2 ± 0.6 µmol/mg vs. 2.1 ± 0.3 µmol/mg). Hence, the acetate formed from methane capture using ANME-1 Mcr is readily converted by the host methanogen into ethanol, and the host can form ethanol without cloned ANME-1 Mcr, although at lower levels, via the host Mcr that primarily produces methane.

Confirming methane utilization via ANME-1, methane consumption at day 6 was higher for C2A/pES1-MAT*mcr3* (11 ± 2%, corresponding to 130 ± 30 µmol) compared to C2A/pES1(Pmat) (6.2 ± 0.8%, corresponding to 71 ± 9 µmol) (Fig. 1B). As expected, vials lacking cells failed to consume methane, confirming no abiotic methane losses. These results show methane was primarily consumed by active ANME-1 Mcr (Fig. 1B).

Iron(III) increases ethanol production with ANME-1 Mcr

Growth of *M. acetivorans* on methane proceeds via iron reduction since the electrons of methane must be transferred to an external acceptor (**Eqn 1**)[6]; hence, to explore the role of iron in ethanol production, the vials were supplemented with 10 mM $FeCl_3$. Iron(III) addition had little influence on methane consumption by C2A/pES1-MAT*mcr3* (13 ± 3% vs. 11 ± 2%) and C2A/pES1(Pmat) (7.6 ± 0.9% vs. 6.2 ± 0.8%) (Fig. 1B); however, ethanol production by C2A/pES1-MAT*mcr3* was significantly higher in presence of iron(III) (Fig. 1A, 180 ± 20 µmol vs. 120 ± 10 µmol) whereas ethanol produced by C2A/pES1(Pmat) was almost similar to that produced in absence of iron (Fig. 1A, 60 ± 20 µmol vs. 50 ± 20 µmol). The ratio of ethanol produced by C2A/pES1-MAT*mcr3* vs. C2A/pES1(Pmat) in presence iron(III) was 3 ± 1 (vs. 2.4 ± 0.9, in absence of iron(III)). Moreover, normalized ethanol was increased in presence of iron(III), by 60 ± 20% for C2A/pES1-MAT*mcr3* (8.1 ± 0.8 µmol/mg vs. 5.2 ± 0.6 µmol/mg) and by 30 ± 30% for C2A/pES1(Pmat) (2.7 ± 0.5 µmol/mg vs. 2.1 ± 0.3 µmol/mg). Thus, supplementing with 10 mM $FeCl_3$ as an external electron acceptor increased ethanol production by *M. acetivorans*.

In the presence of iron(III), the impact of plasmid pES1(Pmat) on host C2A was checked. As expected, we found the ethanol and acetate produced along with the methane consumed by C2A without a plasmid in 6 days at a turbidity of 40 was similar to that with C2A/pES1(Pmat) (Supplementary Fig. S2). These results also confirm that C2A without ANME-1 Mcr is capable of reversing methanogenesis using its native (chromosomal) Mcr to produce ethanol; although the chromosomal Mcr primarily produces methane.

Iron(III) reduces intermediate acetate concentrations

Acetate, the intermediate product between methane and ethanol conversion, was produced at higher concentrations by C2A/pES1-MAT*mcr3* (210 ± 60 µmol) and C2A/pES1(Pmat) (180 ± 80 µmol) without iron(III) (Fig. 1C). However, it was reduced to 120 ± 20 µmol for C2A/pES1-MAT*mcr3* and 40 ± 30 µmol for C2A/pES1(Pmat) when 10 mM iron(III) was added (Fig. 1C). Previously, we used high-cell density cultures to produce acetate from methane in HS medium with 0.1 mM iron(III)[6] and 31 ± 4 µmol of acetate was produced by C2A/pES1(Pmat) and 52 ± 4 µmol of acetate was produced by C2A/pES1-MAT*mcr3* (1.7-fold higher). The decrease in acetate accumulation in presence of iron(III) compared to absence of iron(III) indicates that acetate was more readily converted to ethanol in the presence of iron(III).

Yeast extract and humic acids increase ethanol production

To further increase ethanol production, yeast extract (2.5 g/L) and humic acids (0.1 g/L) were added. Yeast extract stimulates slightly growth of *M. acetivorans* and reduces its lag phase[5,9]. Humic acids facilitate electron transfer from *M. acetivorans* during growth on methane (**Eqn 1**)[15–17]. Additionally, since methane capture previously was shown to occur in biofilms on solid $FeCl_3$ precipitates[6], we further added glass wool (10 g/L) to increase surface area for biofilm formation. Critically, by adding yeast extract and humic acids, ethanol production increased by 110 ± 20% for C2A/pES1-MAT*mcr3* (370 ± 20 µmol) and by 240 ± 90% for C2A/pES1(Pmat) (205 ± 9 µmol) (Fig. 1A). Likewise, normalized ethanol increased by 110 ± 20% for C2A/pES1-MAT*mcr3* (17 ± 1 µmol/mg) and by 210 ± 50% for C2A/pES1(Pmat) (8.4 ± 0.6 µmol/mg). Methane consumption was not much influenced (Fig. 1B) by these two additives. C2A/pES1-MAT*mcr3* (15 ± 3% vs. 13 ± 3%) consistently showed higher methane capture compared to C2A/pES1(Pmat) (11 ± 2% vs. 7.6 ± 0.9%) (Fig. 1B).

Increasing solid surface area does not increase ethanol production

Contrary to our expectations, glass wool was found to be not necessary for improving ethanol production (Fig. 1A) and methane consumption (Fig. 1B). Additionally, we attempted to improve ethanol production by increasing the solid $FeCl_3$ precipitates for biofilm formation by increasing iron(III) concentration from 10 mM to 100 mM. Unfortunately, high iron(III) concentrations was deleterious as ethanol production was reduced by 66 ± 6% for C2A/pES1-MAT*mcr3* (130 ± 10 µmol vs. 370 ± 20 µmol) and by 79 ± 6% for C2A/pES1(Pmat) (43 ± 4 µmol vs. 205 ± 9 µmol) (Fig. 1A). Methane consumption was reduced slightly (C2A/pES1-MAT*mcr3*, 12 ± 2% vs. 15 ± 3%; C2A/pES1(Pmat), 7.9 ± 0.3% vs. 11 ± 2%) (Fig. 1B). Corroborating this, acetate production was also reduced for both C2A/pES1-MAT*mcr3* (by 60 ± 20%, 30 ± 10 µmol vs. 80 ± 10 µmol) and C2A/pES1(Pmat) (by 70 ± 30%, 30 ± 10 µmol vs. 130 ± 30 µmol). Moreover, we found that although the medium was buffered with 50 mM PIPES, the final pH of both the cultures was very low (less than 2) with 100 mM iron(III) whereas the final pH of the cultures with 10 mM $FeCl_3$ was ~6. Thus, the highly acidic culture condition with 100 mM iron(III) was detrimental for the cells which further reduced the conversion of methane to ethanol. Hence, these results demonstrate that the surface area provided by the 10 mM $FeCl_3$ precipitates already provides a sufficient surface area for capturing methane by Mcr3 and converting it to ethanol.

Methane is the primary carbon source for ethanol produced via ANME-1 Mcr

Since ethanol was produced in the absence of ANME-1 Mcr (in C2A/pES1(Pmat), Fig. 1A), we further performed several control experiments without methane to support our finding that ethanol is primarily being produced from methane in C2A/pES1-MAT*mcr3*. We also evaluated the exact contribution of yeast extract and humic acids towards ethanol production in both C2A/pES1-MAT*mcr3* and C2A/pES1(Pmat). In the absence of methane, 150 ± 10 and 124 ± 3 µmol of ethanol was respectively produced by C2A/pES1-MAT*mcr3* and C2A/pES1(Pmat) at a turbidity of 40 in

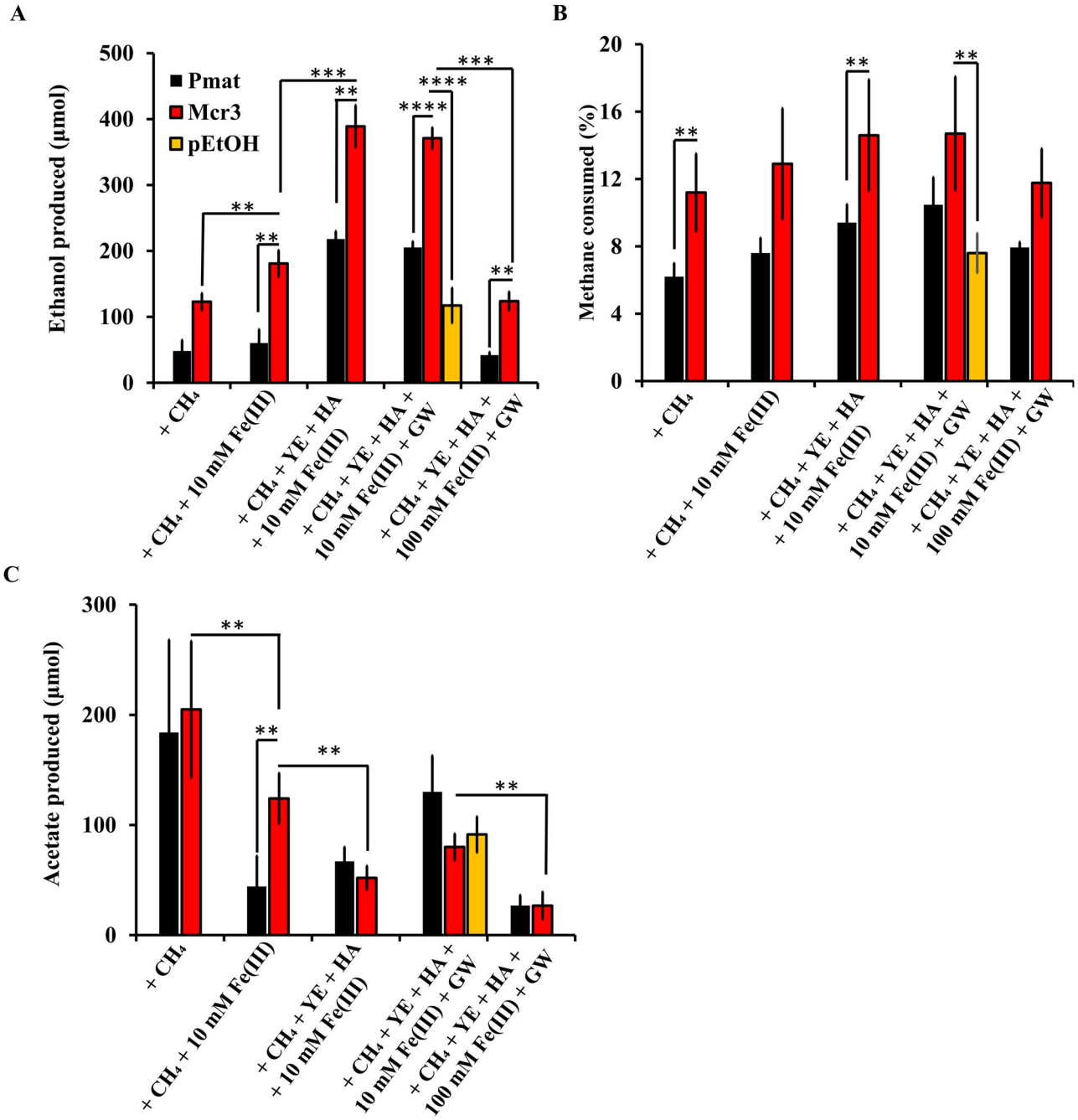

Fig. 1 | Analysis of ethanol and acetate produced and methane consumed by engineered *M. acetivorans* at a turbidity of 40 after 6 days of incubation shows ANME-1 Mcr can drive biofuel production. A Ethanol produced by engineered *M. acetivorans* strains. **B** Methane consumed by the engineered *M. acetivorans* strains. **C** Intermediate acetate produced by the engineered *M. acetivorans* strains. Pmat represents C2A/pES1(Pmat), Mcr3 represents C2A/pES1-MAT*mcr3*, and pEtOH represents C2A/pES1-EtOH. "+ CH_4" indicates presence of headspace methane, "+ Fe(III)" indicates addition of 10 mM $FeCl_3$, "+ YE" indicates addition of 2.5 g/L yeast extract (YE), "+ HA" indicates addition of 0.1 g/L humic acids (HA), "+ GW" indicates addition of 10 g/L glass wool, and "100 mM Fe(III) indicates addition of 100 mM $FeCl_3$. Ethanol, methane, and acetate measurements are from separate samples, and bars and error bars are the mean and standard deviation of three independent cultures. **p < 0.05, ***p < 0.005, ****p < 0.0005. Additional controls are shown in Supplementary Fig. S3.

control vials containing yeast extract, humic acids and 10 mM $FeCl_3$, after 6 days of incubation (Supplementary Fig. S3). Critically, we noted that C2A/pES1-MAT*mcr3* and C2A/pES1(Pmat) produced similar levels of ethanol, indicating that ANME-1 *mcrBGA* are non-functional in absence of methane, as expected. Ethanol produced in the absence of methane was from yeast extract and humic acids since only low levels of ethanol were formed in vials lacking yeast extract, humic acids, and methane (Supplementary Fig. S3, C2A/pES1-MAT*mcr3*, 9 ± 7 µmol; C2A/pES1(Pmat), 19 ± 4 µmol). In vials containing only yeast extract, ethanol produced by C2A/pES1-MAT*mcr3* was 54 ± 4 µmol and by C2A/pES1(Pmat) was 60 ± 20 µmol (Supplementary Fig. S3). Similarly, in vials containing only humic acids, ethanol produced by C2A/pES1-MAT*mcr3* was 50 ± 10 µmol, and by C2A/pES1(Pmat) was 30 ± 10 µmol (Supplementary Fig. S3). Altogether, we estimate, based on the assumption that the metabolic flux from different sources is additive, that approximately 69 ± 5% of the total ethanol produced by C2A/pES1-MAT*mcr3* (370 ± 20 µmol) is contributed by methane, 15 ± 1% is contributed by yeast extract, 13 ± 4% is contributed by humic acids, and 3 ± 2% is coming from some other unknown source (Supplementary Table S2). For

C2A/pES1(Pmat) (205 ± 9 µmol), we estimate that approximately 50 ± 10% is contributed by methane, 30 ± 10% is contributed by yeast extract, 16 ± 6% is contributed by humic acids, and 9 ± 2% is coming from some other unknown source (Supplementary Table S2).

Further engineering of *M. acetivorans* does not improve ethanol production

We further engineered the *M. acetivorans* chassis to improve ethanol production from methane by adding *car* encoding carboxylic acid reductase from *Moorella thermoacetica*[18] and *adh* encoding alcohol dehydrogenase from *Synechocystis* sp. PCC 6803[19] to ANME-1 *mcrBGA* to *M. acetivorans* C2A using vector pES1 to form C2A/pES1-EtOH, which expresses *car*, *adh*, and *mcrBGA* using the ANME-1 promoter $P_{mcr\_ANME\text{-}1}$[6] (Supplementary Fig. S1C). Under the best ethanol producing condition (medium supplemented with headspace methane at 1 atm, 2.5 g/L yeast extract, 0.1 g/L humic acids, and 10 mM iron (III)) and in presence of glass wool (10 g/L), we assayed methane consumption, ethanol, and acetate production by C2A/pES1-EtOH at a turbidity of 40 and compared with C2A/pES1-MAT*mcr3* and C2A/pES1(Pmat). We further prolonged the incubation period to 12 days and then sonicated the cells to determine its effect on ethanol yield. Unfortunately, after 6 days of incubation, the ethanol by C2A/pES1-EtOH was lowest (120 ± 30 µmol) compared to C2A/pES1-MAT*mcr3* (370 ± 20 µmol) and C2A/pES1(Pmat) (205 ± 9 µmol) (Fig. 1A). Moreover, ethanol production did not increase and showed a similar trend after 12 days of incubation (C2A/pES1-MAT*mcr3*, 360 ± 10 µmol; C2A/pES1-EtOH, 100 ± 40 µmol; C2A/pES1(Pmat), 230 ± 10 µmol).

Consistently, methane consumption by C2A/pES1-EtOH was lower (8 ± 1%, corresponding to 90 ± 10 µmol) compared to C2A/pES1-MAT*mcr3* (15 ± 3%) and C2A/pES1(Pmat) (11 ± 2%) (Fig. 1B) at day 6. Likewise, we found that sonication after 12 days to release any intracellular ethanol was not beneficial and ethanol amounts remained almost unchanged (C2A/pES1-MAT*mcr3*, 330 ± 30 µmol; C2A/pES1-EtOH, 90 ± 40 µmol; C2A/pES1(Pmat), 210 ± 30 µmol). At day 6, acetate production by C2A/pES1-EtOH (90 ± 20 µmol) was higher compared to C2A/pES1-MAT*mcr3* (80 ± 10 µmol) but lower than C2A/pES1(Pmat) (130 ± 30 µmol). The acetate levels remained almost similar after 12 days of incubation (C2A/pES1(Pmat), 140 ± 30 µmol; C2A/pES1-MAT*mcr3*, 100 ± 30 µmol; C2A/pES1-EtOH, 90 ± 30 µmol). Like ethanol, sonication made little difference in acetate production (C2A/pES1-EtOH, 70 ± 30 µmol; C2A/pES1-MAT*mcr3*, 80 ± 20 µmol; C2A/pES1(Pmat), 120 ± 50 µmol), indicating that both acetate and ethanol were primarily exported. Altogether, we discovered that the methanogenic host, C2A/pES1-MAT*mcr3* converts acetate into ethanol more efficiently than our heterologous biosynthetic pathway utilizing possibly the AOR/Adh pathway of the host[20].

Time course of ethanol production from methane

Using the two key strains, C2A/pES1(Pmat) and C2A/pES1-MAT*mcr3* at a turbidity of 40, and the optimal conditions for ethanol production (medium supplemented with headspace methane at 1 atm, 2.5 g/L yeast extract, 0.1 g/L humic acids, and 10 mM iron(III) in the absence of glass wool), we assayed methane consumption along with ethanol and acetate production over 8 days (Fig. 2) to corroborate and provide additional details for the 6-day results of Fig. 1. We found ethanol production gradually increased up to day 6 (Fig. 2A): C2A/pES1-MAT*mcr3* produced 400 ± 40 µmol of ethanol vs. 210 ± 10 µmol by C2A/pES1(Pmat). Up to 18 ± 3% (210 ± 30 µmol) of methane was consumed by C2A/pES1-MAT*mcr3* in 8 days which was ~2-fold higher than that of C2A/pES1(Pmat) (8 ± 1%; 90 ± 20 µmol) (Fig. 2B). Intermediate acetate accumulated by C2A/pES1-MAT*mcr3* decreased after Day 4, indicating that the acetate was converted to ethanol (Fig. 2C). Hence, the time-course data corroborate well the 6-day methane-to-ethanol results of Fig. 1.

Identification of candidate genes involved in ethanol production from acetate

From RNA sequencing data of the differential gene analysis of C2A/pES1-MAT*mcr3* for cells grown on methane vs. cells grown in methanol[6], we identified induced genes that might be involved in the conversion of acetate to ethanol (Fig. 3), including genes encoding AOR (MA_2962), ferredoxin (MA_0463), 4Fe-4S ferredoxin-type domain-containing proteins (MA_3299, MA_4249, MA_4242, MA_0739, MA_4409, and MA_4241), and tungsten-containing aldehyde ferredoxin oxidoreductase cofactor modifying protein (MA_0794) (Table 1). In the thermophilic archaeon *Pyrococcus furiosus*, the conversion of acetate to acetaldehyde is catalyzed by AOR encoded by PF0346[20]. AOR from MA_2962 has 30% identity with the AOR of *P. furiosus* and was sharply induced during growth on methane (Table 1), so the likely host enzyme for acetate to acetaldehyde is AOR (MA_2962) (Fig. 3).

The second step, i.e., acetaldehyde to ethanol is catalyzed by alcohol dehydrogenase. In *P. furiosus*, introduction of *adhA* from *Thermoanaerobacter* strain X514 enabled ethanol production by the engineered strain[20]. For growth of C2A/pES1-MAT*mcr3* on methane vs. on methanol, the RNA seq data showed that gene encoding Adh (MA_0403) was induced three-fold, so the likely host enzyme for acetaldehyde to ethanol in *M. acetivorans* is Adh (MA_0403).

Thermodynamic analysis suggests ferredoxin-dependent ethanol generation

Energetic considerations also corroborate that host reduced ferredoxin may act as the electron donor for reducing acetate to acetaldehyde by AOR from MA_2962 (Fig. 3). Acetate to acetaldehyde reduction has a standard redox potential $E_0' \approx -580$ mV[21], but the E_0' NADH/NAD^+ is ≈ −320 mV and thus NADH/NAD^+ might not drive the reduction of acetate to acetaldehyde. E_0' for reduced ferredoxin is ≈ −500 mV and thus might serve as the electron donor for acetate reduction to acetaldehyde by AOR (MA_2962)[21]. Moreover, in anaerobic metabolism, ferredoxin plays a central role in electron transfer[22]. Hence, the induction of 4Fe-4S electron transfer proteins (Table 2) for growth on methane, indicates that the reduction of acetate to ethanol might be ferredoxin dependent.

In addition, prior mechanistic work proposed an electron-bifurcating complex (EBC) that couples oxidation of HSCoM/HSCoB to both iron(III) reduction and ferredoxin reduction[6]. This mechanism provides the reducing power necessary for the mildly endergonic acetate-to-acetaldehyde step ($\Delta G^{o\prime} \approx +46$ kJ/mol)[21] (Table 2). The subsequent aldehyde reduction to ethanol is favorable ($\Delta G^{o\prime} \approx -23.2$ kJ/mol) (Table 2), yielding a slightly endergonic net conversion of acetate to ethanol ($\Delta G^{o\prime} \approx +22.8$ kJ/mol)[20]. Thus, the highly favorable methane oxidation step by cloned ANME-1 Mcr supplies the thermodynamic leverage required to drive the downstream acetate-to ethanol reactions ($\Delta G^{o\prime} \approx -570.3$ kJ/mol CH_4, Table 2).

The behavior observed experimentally aligns with this model. Iron(III) addition enhances ethanol production by increasing electron flux through the iron(III)-coupled respiratory chain, supporting both ferredoxin reduction and ATP generation[6]. In contrast, excessive iron(III) concentrations disrupt this balance by acidifying the medium, shifting proton-consuming reductions into unfavorable regimes and lowering acetate and ethanol production. Overall, the thermodynamic considerations demonstrate that strongly exergonic methane oxidation drives acetyl-CoA and acetate formation, while iron(III)-supported ferredoxin reduction enables the otherwise unfavorable reduction of acetate to ethanol, establishing a coherent and thermodynamically feasible route for biological methane conversion to ethanol.

Stochiometric analysis shows good agreement for methane conversion to ethanol

According to the overall stoichiometric equation for methane to ethanol (Table 2), 4 moles of methane and 2 moles of carbonate yield 3 moles of ethanol. Using methane as the sole carbon source without iron(III), the methane captured by C2A/pES1-MAT*mcr3* in 6 days was 130 ± 30 µmol (11 ± 2% in Fig. 1B) and by C2A/pES1(Pmat) was 71 ± 9 µmol (6.2 ± 0.8% in Fig. 1B), so the theoretical ethanol yield is 100 ± 20 µmol for C2A/pES1-MAT*mcr3* and 53 ± 7 µmol for C2A/pES1(Pmat). Therefore, ethanol produced from C2A/pES1-MAT*mcr3* (120 ± 10 µmol) and C2A/pES1(Pmat) (50 ± 20 µmol) (Fig. 1A) closely correlated with the theoretical yields.

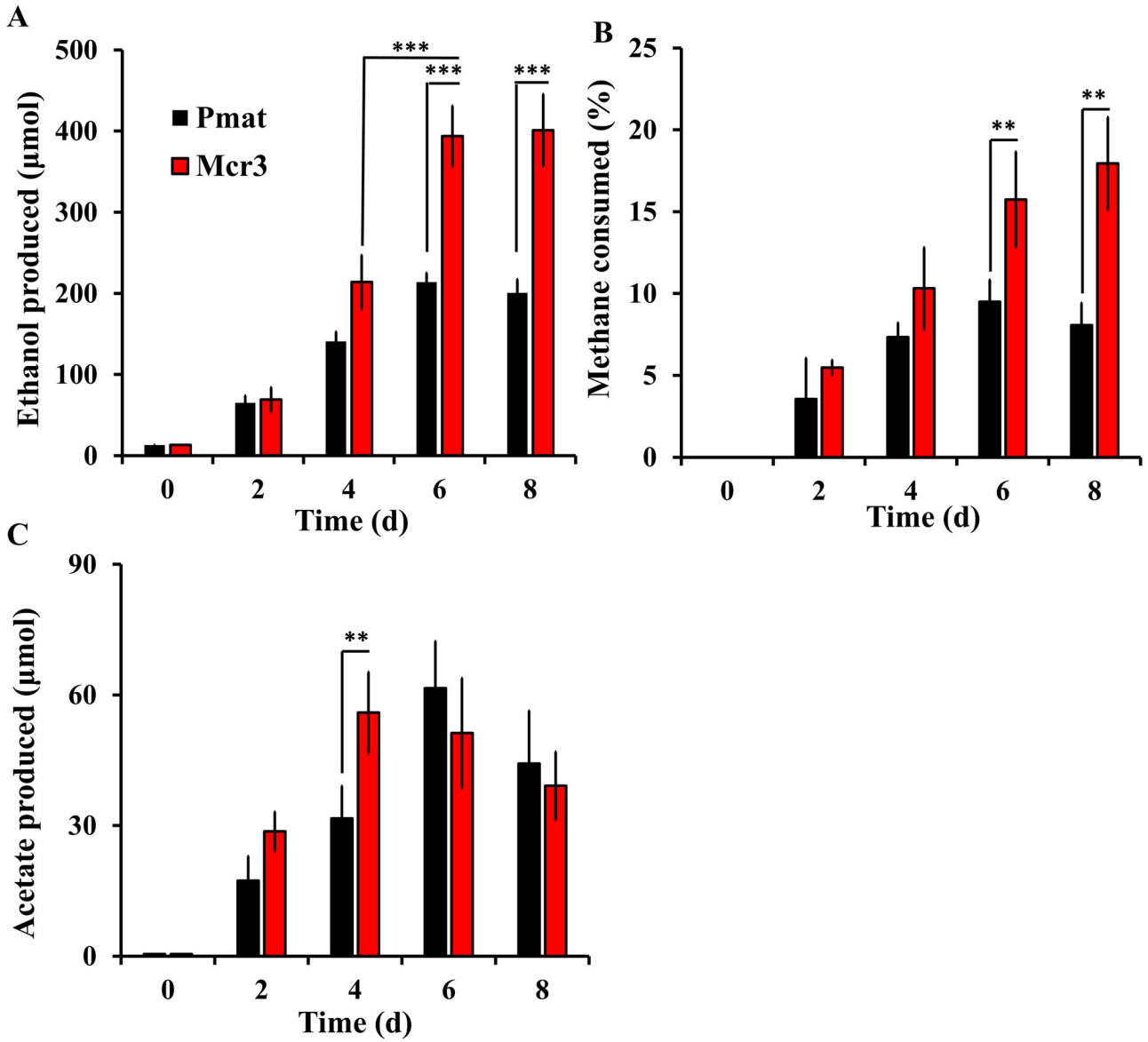

Fig. 2 | Time course of ethanol and acetate produced from captured methane by engineered *M. acetivorans* at a turbidity of 40 under optimal ethanol producing conditions (medium supplemented with headspace methane at 1 atm, 2.5 g/L yeast extract, 0.1 g/L humic acids, and 10 mM iron(III) in the absence of glass wool) over a period of 8 days. A Ethanol produced by engineered *M. acetivorans* strains. **B** Methane consumed by the engineered *M. acetivorans* strains. **C** Intermediate acetate produced by the engineered *M. acetivorans* strains. Pmat represents C2A/pES1(Pmat), and Mcr3 represents C2A/pES1-MAT*mcr3*. Bars and error bars are the mean and standard deviation of three independent cultures. ** $p < 0.05$, *** $p < 0.005$.

Carbon mass balance analysis showed that 130 ± 30% of the carbon from the captured methane was recovered in the ethanol produced by C2A/pES1-MAT*mcr3* (Supplementary Table S3). The carbon recovery for the ethanol produced by C2A/pES1(Pmat) was 90 ± 30% (Supplementary Table S3). The electrons released during methane oxidation was recovered by 100 ± 20% in the ethanol produced by C2A/pES1-MAT*mcr3* and by 70 ± 30% for C2A/pES1(Pmat) (Supplementary Table S3). Similarly, in the presence of 10 mM iron(III), there was good agreement between the theoretical and experimental yields: methane captured in 6 days was 150 ± 40 μmol for C2A/pES1-MAT*mcr3* (13 ± 3% in Fig. 1B) and 90 ± 10 μmol for C2A/pES1(Pmat) (7.6 ± 0.9%, Fig. 1B), and the ethanol produced from C2A/pES1-MAT*mcr3* (180 ± 20 μmol) and C2A/pES1(Pmat) (60 ± 20 μmol) (Fig. 1A) correlated with the theoretical yields (C2A/pES1-MAT*mcr3*, 110 ± 30 μmol; C2A/pES1(Pmat), 65 ± 8 μmol). The carbon recovery was 160 ± 50% for the ethanol produced by C2A/pES1-MAT*mcr3* and 90 ± 30% for C2A/pES1(Pmat) (Supplementary Table S3). The electrons recovered was 150 ± 40% for C2A/pES1-MAT*mcr3* and 90 ± 30% for C2A/pES1(Pmat) (Supplementary Table S3). Hence, our results validate the balanced stoichiometric equation, highlighting C2A/pES1-MAT*mcr3* as an efficient system for methane to ethanol conversion.

Discussion

Our results demonstrate that ethanol can be produced from methane and carbon dioxide by engineered *M. acetivorans* producing ANME-1 Mcr. We found that the ethanol that is produced is (i) two-fold higher than the host without the cloned ANME-1 Mcr, (ii) additives such as iron(III), yeast extract and humic acids increase ethanol production from methane by three-fold (Fig. 1A), (iii) 10 mM iron provides sufficient surface area needed for capturing methane by ANME-1 Mcr (with 100 mM iron having a deleterious effect), and (iv) the methanogenic host is capable of converting the intermediate acetate to ethanol most likely via native AOR/Adh (Fig. 3). Therefore, this methanogenic host forms an efficient platform for ethanol production from the acetate derived from the ANME-1 Mcr captured methane.

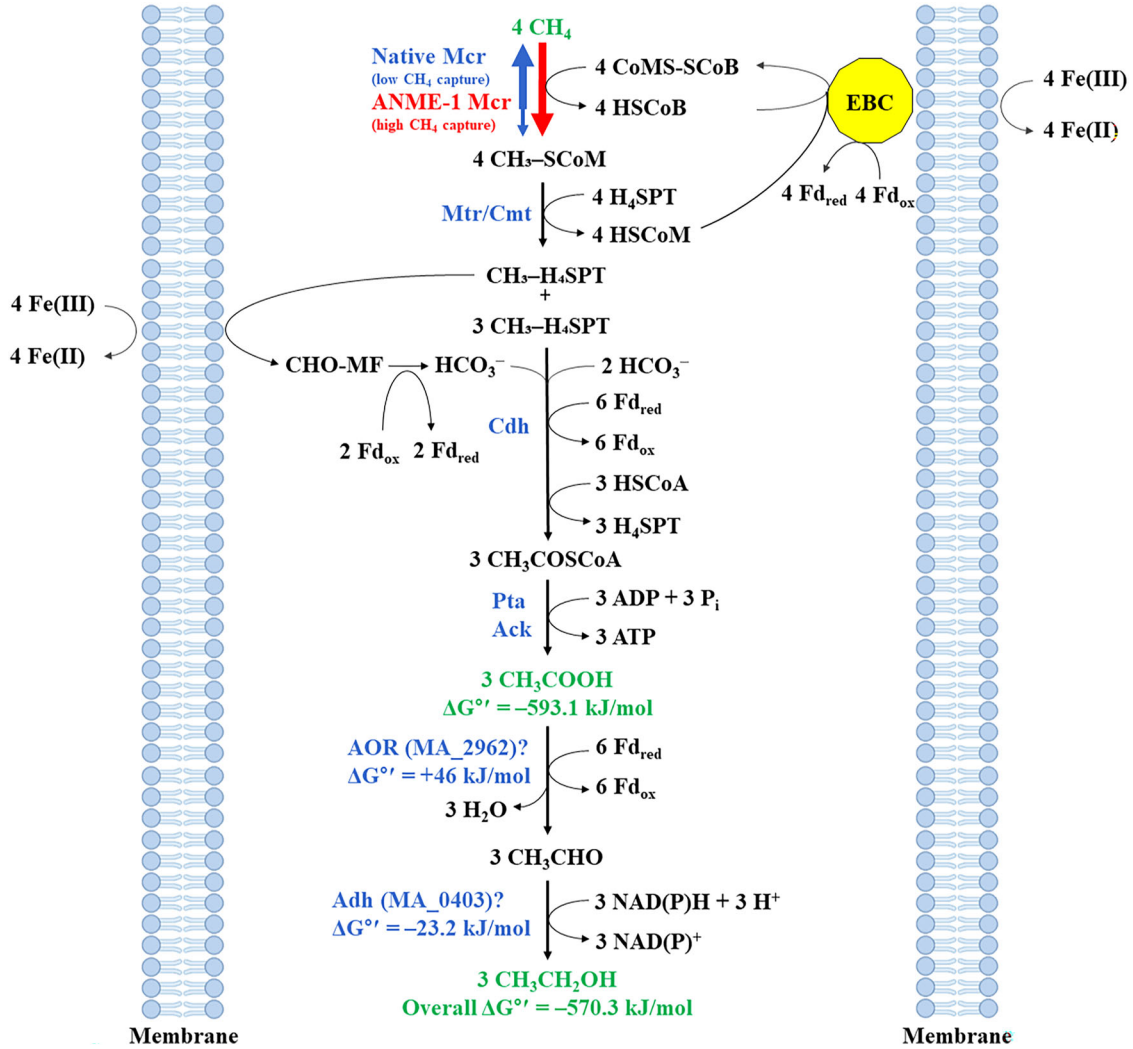

Fig. 3 | Probable metabolic pathway for ethanol production from methane. Native **enzymes** of the host are indicated in blue and cloned ANME-1 Mcr is indicated in red: EBC, electron-bifurcating complex; Mtr, membrane-bound methyltransferase; Cmt, cytoplasmic methyltransferase; Cdh, carbon monoxide dehydrogenase complex; Pta, phosphotransacetylase; Ack, acetate kinase. '?' indicates probable enzymes used by the host for converting acetate into ethanol. **Metabolites**: CH_4, methane; CoMS-SCoB, heterodisulfide of coenzyme M and coenzyme B; HSCoB, coenzyme B; CH_3-SCoM, methyl-coenzyme M; H_4SPT, 5,6,7,8-tetrahydrosarcinapterin; HSCoM, coenzyme M; Fd_{red}, reduced ferredoxin; Fd_{ox}, oxidized ferredoxin; CH_3-H_4SPT, methyl-5,6,7,8-tetrahydrosarcinapterin; CHO-MF, formyl methanofuran; HCO_3^-, bicarbonate ion; HSCoA, coenzyme A; $CH_3COSCoA$, acetyl-CoA; ADP, adenosine diphosphate; P_i, inorganic phosphate; ATP, adenosine triphosphate; CH_3COOH, acetic acid; H_2O, water; CH_3CHO, acetaldehyde; NAD(P)H, nicotinamide adenine dinucleotide phosphate, reduced form; H^+, hydrogen ion; $NAD(P)^+$, nicotinamide adenine dinucleotide phosphate, oxidized form; CH_3CH_2OH, ethanol.

Table 1 | Candidate induced genes involved in acetate to ethanol conversion by C2A/pES1-MAT*mcr3* for growth on methane vs. growth on methanol

Step	Candidate genes	Fold induction (CH_4 vs. CH_3OH)	Gene product
Acetate to acetaldehyde	MA_0794	12.2	Tungsten-containing aldehyde ferredoxin oxidoreductase cofactor modifying protein
	MA_2962	∞	Aldehyde ferredoxin oxidoreductase
	MA_0463	9.6	Ferredoxin
	MA_3299	∞	4Fe-4S ferredoxin-type domain-containing protein
	MA_4249	2.7	4Fe-4S ferredoxin-type domain-containing protein
	MA_4242	1.5	4Fe-4S ferredoxin-type domain-containing protein
	MA_0739	1.3	4Fe-4S ferredoxin-type domain-containing protein
	MA_4409	1.2	4Fe-4S ferredoxin-type domain-containing protein
Acetaldehyde to ethanol	MA_0403	3	Zinc-binding alcohol dehydrogenase
	MA_1321	∞	Short chain dehydrogenase

Table 2 | Thermodynamic properties of the methane-to-ethanol pathway in *M. acetivorans*. Standard Gibbs free energies ($\Delta G^{\circ\prime}$) are expressed under biochemical standard conditions (pH 7, 25 °C, 1 atm) and are normalized per reaction as written (4 mol CH_4 basis)

Step	Reaction	Catalyzed by	$\Delta G^{\circ\prime}$, kJ/mol	References
Methane → acetate	$4\ CH_4 + 2\ HCO_3^- + 8\ Fe^{3+} + 3\ ADP + 3\ P_i \rightarrow 3\ CH_3COO^- + 8\ Fe^{2+} + 9\ H^+ + 3\ ATP$	ANME-1 Mcr	–593.1	6
Acetate → acetaldehyde	$3\ CH_3COO^- + 6\ Fd_{red} + 9\ H^+ \rightarrow 3\ CH_3CHO + 6\ Fd_{ox} + 3\ H_2O$	AOR	+46	18
Acetaldehyde → ethanol	$3\ CH_3CHO + 3\ NAD(P)H + 3\ H^+ \rightarrow 3\ CH_3CH_2OH + 3\ NAD(P)^+$	Adh	–23.2	18
Overall CH_4 → ethanol	$4\ CH_4 + 2\ HCO_3^- + 8\ Fe^{3+} + 6\ Fd_{red} + 3\ NAD(P)H + 3\ H^+ + 3\ ADP + 3\ P_i \rightarrow 3\ CH_3CH_2OH + 8\ Fe^{2+} + 6\ Fd_{ox} + 3\ NAD(P)^+ + 3\ H_2O + 3\ ATP$		–570.3	6,18

For Step 1, the reported chemical standard-state free energy ($\Delta G^{\circ}{}'_{rxn} = -325$ kJ/mol)[6] was transformed to $\Delta G^{\circ\prime}$ by accounting for proton activity at pH 7 ($\Delta nH^+ = +9$): $\Delta G^{\circ\prime} = \Delta G^{\circ} + RT\ln([H^+]^9)$. ATP synthesis was included using $\Delta G^{\circ\prime} = +30.5$ kJ/mol ATP. Steps 2–3 were calculated from literature $E^{\circ\prime}$ values according to $\Delta G^{\circ\prime} = -nF\Delta E^{\circ\prime}$. Mcr is methyl-coenzyme M reductase, AOR is aldehyde ferredoxin oxidoreductase, and Adh is alcohol dehydrogenase.

Intriguingly, our results also clearly indicate that significant amounts of methane are consumed by the methanogen host, based on the ethanol produced in the absence of cloned ANME-1 Mcr; i.e., by C2A/pES1(Pmat) (Fig. 1) and by wild type C2A with no pES1(Pmat) plasmid (Supplementary Fig. S2). Hence, unlike as reported originally that only trace amounts of methane may be consumed by the methanogen host[23], significant amounts of methane may be metabolized by *M. acetivorans*[6,17] by reversing the host Mcr. However, our study clearly demonstrates that the expression of ANME-1 Mcr is beneficial and it enhances methane consumption and ethanol producing ability of *M. acetivorans*. Note that ANME-1 communities in Black Sea sediments typically experience in situ temperatures of 8 to 9 °C and thus, the incubation temperature of 39 °C, which is the optimum temperature for cultivating *M. acetivorans*, may not be optimal for ANME-1 Mcr activity. However, enzyme activities generally increase with temperature. Regardless, enhanced methane capture by C2A/pES1-MAT*mcr3* compared to C2A/pES1(Pmat) or wild type C2A indicates that the ANME-1 Mcr was functional in *M. acetivorans*.

Surprisingly, cloning *car* from *Moorella thermoacetica* and *adh* from *Synechocystis* sp. PCC 6803 into *M. acetivorans* with ANME-1 Mcr is detrimental for ethanol production. Since we found that the anaerobic host likely uses AOR for catalyzing the mildly endergonic conversion of acetate to acetaldehyde, perhaps it is thermodynamically not feasible for the NAD(P)H dependent Car to catalyze this reaction with low redox potential. Additionally, the foreign Adh might impose a metabolic burden on the host as the natively expressed Adh is already functional, or both heterologous Car and Adh are not produced at adequate levels or active. Our PCR verification of plasmid pES1-EtOH only confirms its presence in the host *M. acetivorans* but does not demonstrate heterologous Car and Adh are active. Although previously we demonstrated via FLAG tag and Western blot analysis that ANME-1 Mcr was produced by C2A/pES1-MAT*mcr3*[6], future functional analysis will be important to confirm the activity of Car and Adh.

We also found that simple media optimization helps to enhance the ethanol production significantly. Critically, humic acids contain quinone moieties as functional groups[24], which get reduced and accelerate transmembrane electron shuttles[25], improving metabolic activity of cell[26], and thereby increases ethanol production. Yeast extract provides nutritional benefits to the cell growth by providing B-vitamins, amino acids, minerals and trace elements, which might fuel up the metabolic activity leading to higher production of ethanol[27]. Since the transformed *M. acetivorans* was not from a single colony, variations within the population might exist which could further complicate interpretation of the phenotype. For future research, significant optimization to increase methane consumption for scale-up, and functional and biochemical analysis to directly address whether the recombinant proteins are stable and whether their subunits are correctly assembled into an active complex, is required. Nevertheless, since the organisms responsible for anaerobic oxidation of methane cannot be cultured as pure cultures (note an exception is the engineered methanogen producing ANME-1 Mcr[6]) and since aerobic organisms produce primarily methanol, not ethanol, our work is important for converting methane into ethanol biologically.

Data availability

Data used in this manuscript are available at on Figshare under the identifier https://doi.org/10.6084/m9.figshare.32065350.

Received: 19 January 2026; Accepted: 29 April 2026;
Published online: 09 May 2026

References

1. Tucci, F. J. & Rosenzweig, A. C. Direct Methane Oxidation by Copper- and Iron-Dependent Methane Monooxygenases. *Chem. Rev.* **124**, 1288–1320 (2024).
2. Friedlingstein, P. et al. Global Carbon Budget 2025. *Earth Syst. Sci. Data Discuss.* **2025**, 1–139 (2025).
3. Wood, T. K., Gurgan, I., Howley, E. T. & Riedel-Kruse, I. H. Converting methane into electricity and higher-value chemicals at scale via anaerobic microbial fuel cells. *Renew. Sustain. Energy Rev.* **188**, 113749 (2023).
4. Knittel, K. & Boetius, A. Anaerobic oxidation of methane: progress with an unknown process. *Annu. Rev. Microbiol.* **63**, 311–334 (2009).
5. Sowers, K. R., Baron, S. F. & Ferry, J. G. *Methanosarcina acetivorans* sp. nov., an acetotrophic methane-producing bacterium isolated from marine sediments. *Appl. Enviro. Microbiol.* **47**, 971–978 (1984).
6. Soo, V. W. C. et al. Reversing methanogenesis to capture methane for liquid biofuel precursors. *Microb. Cell Fact.* **15**, 11 (2016).
7. Kohler, P. R. & Metcalf, W. W. Genetic manipulation of *Methanosarcina* spp. *Front. Microbiol.* **3**, 259 (2012).
8. Woods, P. H. et al. Convergence and horizontal gene transfer drive the evolution of anaerobic methanotrophy in archaea. *bioRxiv*, 2024.2005.2023.595608 (2024).
9. McAnulty, M. J. et al. Metabolic engineering of *Methanosarcina acetivorans* for lactate production from methane. *Biotechnol. Bioeng.* **114**, 852–861 (2017).
10. Smith, W. P. Epidermal and dermal effects of topical lactic acid. *J. Am. Acad. Dermatol.* **35**, 388–391 (1996).
11. Datta, R., Tsai, S. P., Bonsignore, P., Moon, S. H. & Frank, J. R. Technological and economic-potential of poly(lactic acid) and lactic-acid derivatives. *FEMS Microbiol. Rev.* **16**, 221–231 (1995).
12. Wee, Y. J., Kim, J. N. & Ryu, H. W. Biotechnological production of lactic acid and its recent applications. *Food Technol. Biotech.* **44**, 163–172 (2006).
13. Upadhyaya, B. P., DeVeaux, L. C. & Christopher, L. P. Metabolic engineering as a tool for enhanced lactic acid production. *Trends Biotechnol.* **32**, 637–644 (2014).
14. Yamasaki, R., Maeda, T. & Wood, T. K. Electron carriers increase electricity production in methane microbial fuel cells that reverse methanogenesis. *Biotechnol. Biofuels* **11**, 211 (2018).
15. McAnulty, M. J. et al. Electricity from methane by reversing methanogenesis. *Nat. Commun.* **8**, 15419 (2017).
16. Ruebush Shane, S., Brantley Susan, L. & Tien, M. Reduction of Soluble and Insoluble Iron Forms by Membrane Fractions of

Shewanella oneidensis Grown under Aerobic and Anaerobic Conditions. *Appl. Enviro. Microbiol.* **72**, 2925–2935 (2006).
17. Yan, Z. et al. Respiration-driven methanotrophic growth of diverse marine methanogens. *Proc. Natl. Acad. Sci. USA* **120**, e2303179120 (2023).
18. Bertsch, J. & Müller, V. Bioenergetic constraints for conversion of syngas to biofuels in acetogenic bacteria. *Biotechnol. Biofuels* **8**, 210 (2015).
19. Vidal, R., López-Maury, L., Guerrero, M. G. & Florencio, F. J. Characterization of an alcohol dehydrogenase from the Cyanobacterium Synechocystis sp. strain PCC 6803 that responds to environmental stress conditions via the Hik34-Rre1 two-component system. *J. Bacteriol.* **191**, 4383–4391 (2009).
20. Basen, M. et al. Single gene insertion drives bioalcohol production by a thermophilic archaeon. *Proc. Natl. Acad. Sci. USA* **111**, 17618–17623 (2014).
21. Müller, V. Bioalcohol production by a new synthetic route in a hyperthermophilic archaeon. *Proc. Natl. Acad. Sci. USA* **111**, 17352–17353 (2014).
22. Buckel, W. & Thauer, R. K. Flavin-Based Electron Bifurcation, Ferredoxin, Flavodoxin, and Anaerobic Respiration With Protons (Ech) or NAD+ (Rnf) as Electron Acceptors: A Historical Review. *Front. Microbiol.* **9**, 401 (2018).
23. Moran, J. J., House, C. H., Freeman, K. H. & Ferry, J. G. Trace methane oxidation studied in several Euryarchaeota under diverse conditions. *Archaea* **1**, 303–309 (2005).
24. Núñez-Valenzuela, P., Palomo-Briones, R., Cervantes, F. J. & Razo-Flores, E. Humic substances improve the co-production of hydrogen and carboxylic acids by anaerobic mixed cultures. *Int. J. Hydrog. Energy* **46**, 32800–32808 (2021).
25. Lovley, D. R., Coates, J. D., Blunt-Harris, E. L., Phillips, E. J. P. & Woodward, J. C. Humic substances as electron acceptors for microbial respiration. *Nature* **382**, 445–448 (1996).
26. Zhang, L. et al. Enhanced biohydrogen production through dark fermentation by humic acid: insights into microbial composition and functional genes. *J. Microbiol. Biotechnol.* **35**, e2412071 (2025).
27. Li, M., Liao, X., Zhang, D., Du, G. & Chen, J. Yeast extract promotes cell growth and induces production of polyvinyl alcohol-degrading enzymes. *Enzym. Res.* **2011**, 179819 (2011).

Acknowledgements

We thank J. Cuello, R. Sierra Alvarez, and members of the Riedel-Kruse Lab for stimulating discussions. T.K.W. discloses support for the research of this work from the National Science Foundation [NSF-FMRG grant 2229070].

Author contributions

Ruchira Mitra: Investigation, Methodology, Data curation, Writing - original draft, Writing - review & editing. Yunjeong Choi: Investigation, Methodology, Data curation, Writing - review & editing. Hyeon-Ji Hwang: Data curation, writing - review & editing. Rodolfo García-Contreras: Investigation, Methodology. Vanesa Angarita-Zapata: Investigation. Shotaro Toya: Investigation, Methodology. Ilke Gurgan: Investigation, Methodology. Ingmar H. Riedel-Kruse: Project administration, Fund acquisition, Writing - review & editing, Thomas K. Wood: Supervision, Conceptualization, Project administration, Fund acquisition, Writing - original draft, Writing - review & editing.

Competing interests

The authors declare no competing interests.

Additional information

Supplementary information The online version contains supplementary material available at https://doi.org/10.1038/s43247-026-03601-0.

Correspondence and requests for materials should be addressed to Thomas K. Wood.

Peer review information *Communications Earth & Environment* thanks Krishna Sahoo and the other, anonymous, reviewer(s) for their contribution to the peer review of this work. Primary Handling Editors: Heike Langenberg and Marisa McDonald. A peer review file is available.